

SUPPORTING INFORMATION

Ellagic Acid Exerts Dual Action to Curb the Pathophysiological Manifestations of Sickle Cell Disease and Attenuate the Hydroxyurea-Induced Myelosuppression in Berkeley Mice

Abhishek Gour^{†‡}, Dilpreet Kour^{†‡}, Ramajayan Pandian^{†‡}, Mahir Bhardwaj^{†‡}, Sanghapal D. Sawant^{#‡}, Ajay Kumar^{†‡}, Utpal Nandi^{†*}

[†]Pharmacology Division, CSIR-Indian Institute of Integrative Medicine, Jammu-180001, India.

[‡]Academy of Scientific and Innovative Research (AcSIR), Ghaziabad-201002, India.

[#]Natural Products and Medicinal Chemistry Division, CSIR-Indian Institute of Integrative Medicine, Jammu-180001, India.

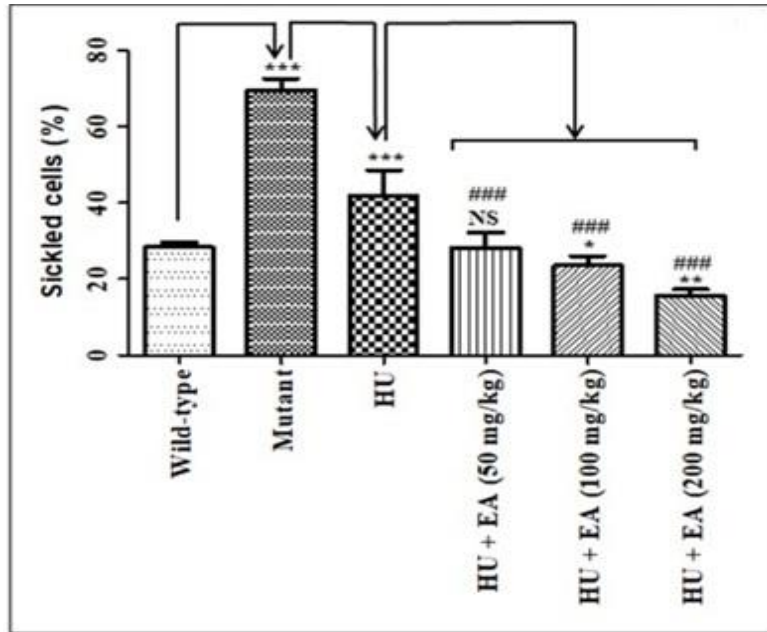


Figure S1. Effect of ellagic acid (EA) upon concomitant treatment with HU on anti-sickling activity. Data are expressed as mean \pm SEM (n=5). $p < 0.05/0.01/0.001$ denotes statistical significance (**/* or ***/###/####). *wild-type vs. mutant/mutant vs. HU/HU vs. HU+EA. #mutant vs. HU+EA. NS denotes not statistically significant.

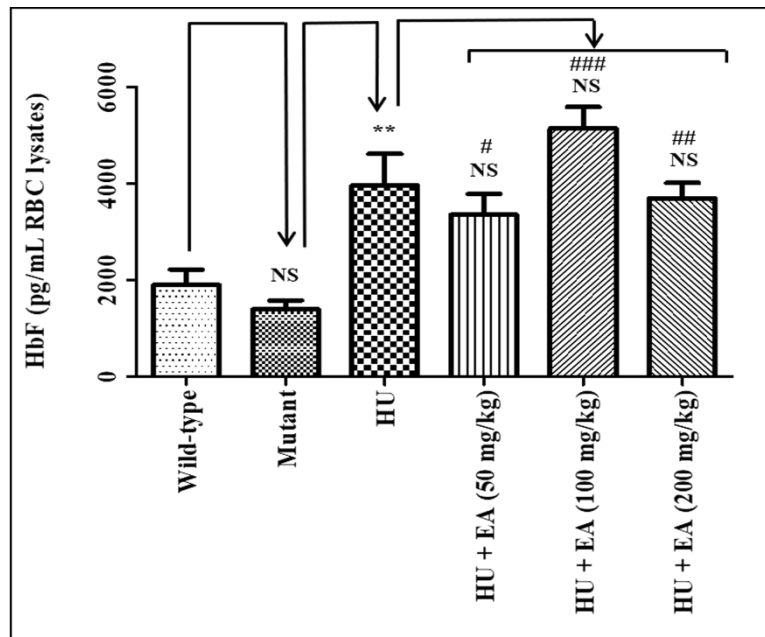


Figure S2. Effect of ellagic acid (EA) upon concomitant treatment with HU on HbF level. Data are expressed as mean \pm SEM (n=5). $p < 0.05/0.01/0.001$ denotes statistical significance (**/* or ***/###/####). *wild-type vs. mutant/mutant vs. HU/HU vs. HU+EA. #mutant vs. HU+EA. NS denotes not statistically significant.

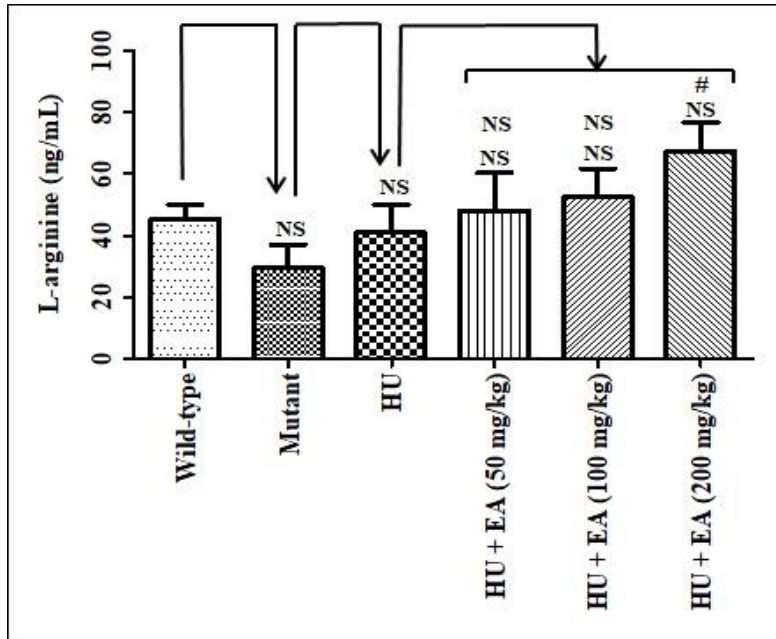


Figure S3. Effect of ellagic acid (EA) upon concomitant treatment with HU on L-arginine level. Data are expressed as mean \pm SEM (n=5). $p < 0.05/0.01/0.001$ denotes statistical significance (*/**/*** or #/##/###). *wild-type vs. mutant/mutant vs. HU/HU vs. HU+EA. #mutant vs. HU+EA. NS denotes not statistically significant.

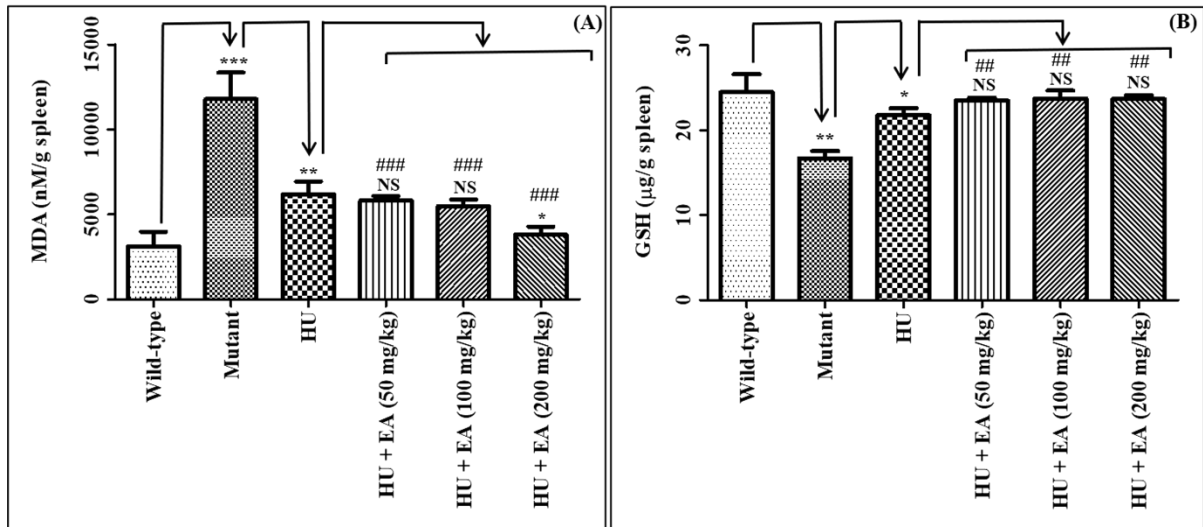


Figure S4. Effect of ellagic acid (EA) upon concomitant treatment with HU on the following parameters: MDA (A); GSH (B). Data are expressed as mean \pm SEM (n=5). $p < 0.05/0.01/0.001$ denotes statistical significance (*/**/*** or #/##/###). *wild-type vs. mutant/mutant vs. HU/HU vs. HU+EA. #mutant vs. HU+EA. NS denotes not statistically significant.

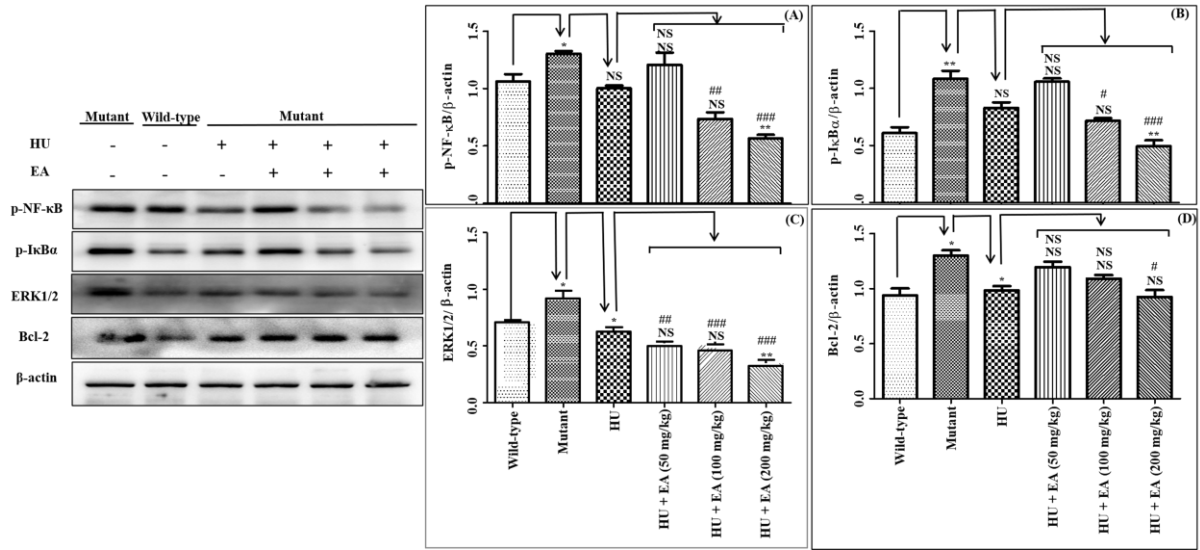


Figure S5. Effect of ellagic acid (EA) upon concomitant treatment with HU on the following parameters: p-NF-κB (A); p-IκBα (B); ERK1/2 (C); Bcl-2 (D). Data are expressed as mean \pm SEM (n=5). $p < 0.05/0.01/0.001$ denotes statistical significance (**/*/* or #/#/#). *wild-type vs. mutant/mutant vs. HU/HU vs. HU+EA. #mutant vs. HU+EA. NS denotes not statistically significant.

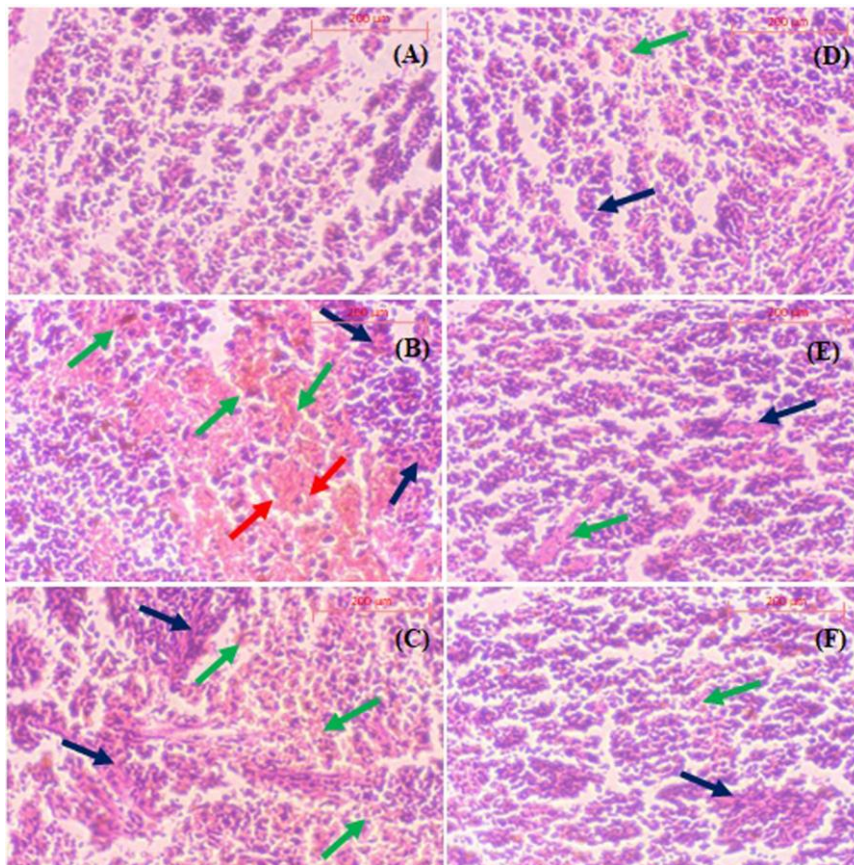


Figure S6. The representative H&E-stained images of the spleen: A for wild-type; B for mutant; C for HU alone; D for HU in combination with ellagic acid (50 mg/kg); E for HU in combination with ellagic acid (100 mg/kg); F for HU in combination with ellagic acid (200 mg/kg). Arrow indicators: Green- RBC congestion; Blue- collagen deposition; Red- vacuolization of histiocytes.

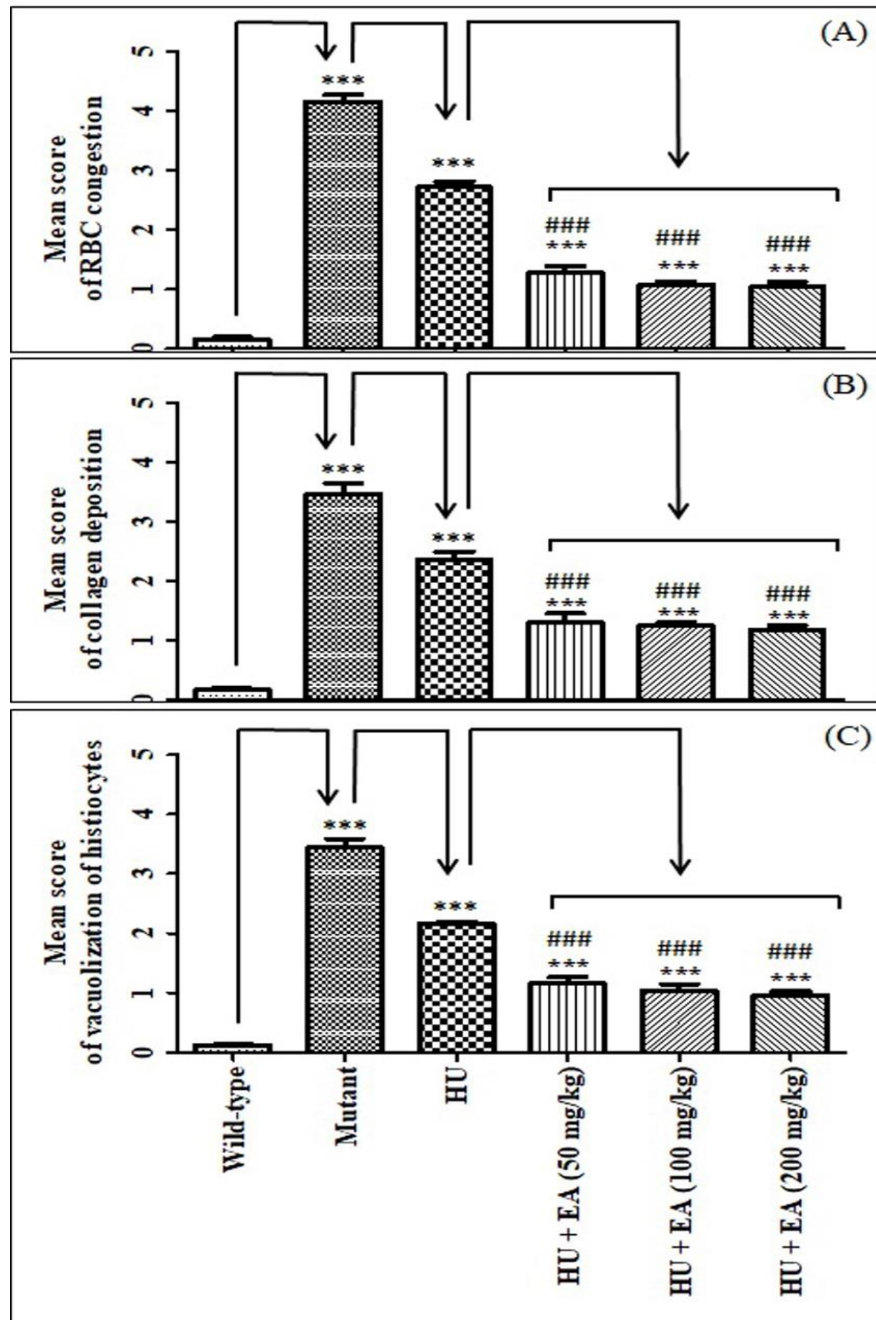


Figure S7. The bar graph for scoring of histopathological features in the spleen among different study groups: RBC congestion (A), collagen deposition (B), and vacuolization of histiocytes (C). Data are expressed as mean \pm SEM (n=5). $p < 0.05/0.01/0.001$ denotes statistical significance (*/**/*** or ###/###/###). *wild-type vs. mutant/mutant vs. HU/HU vs. HU+EA. #mutant vs. HU+EA. NS denotes not statistically significant.

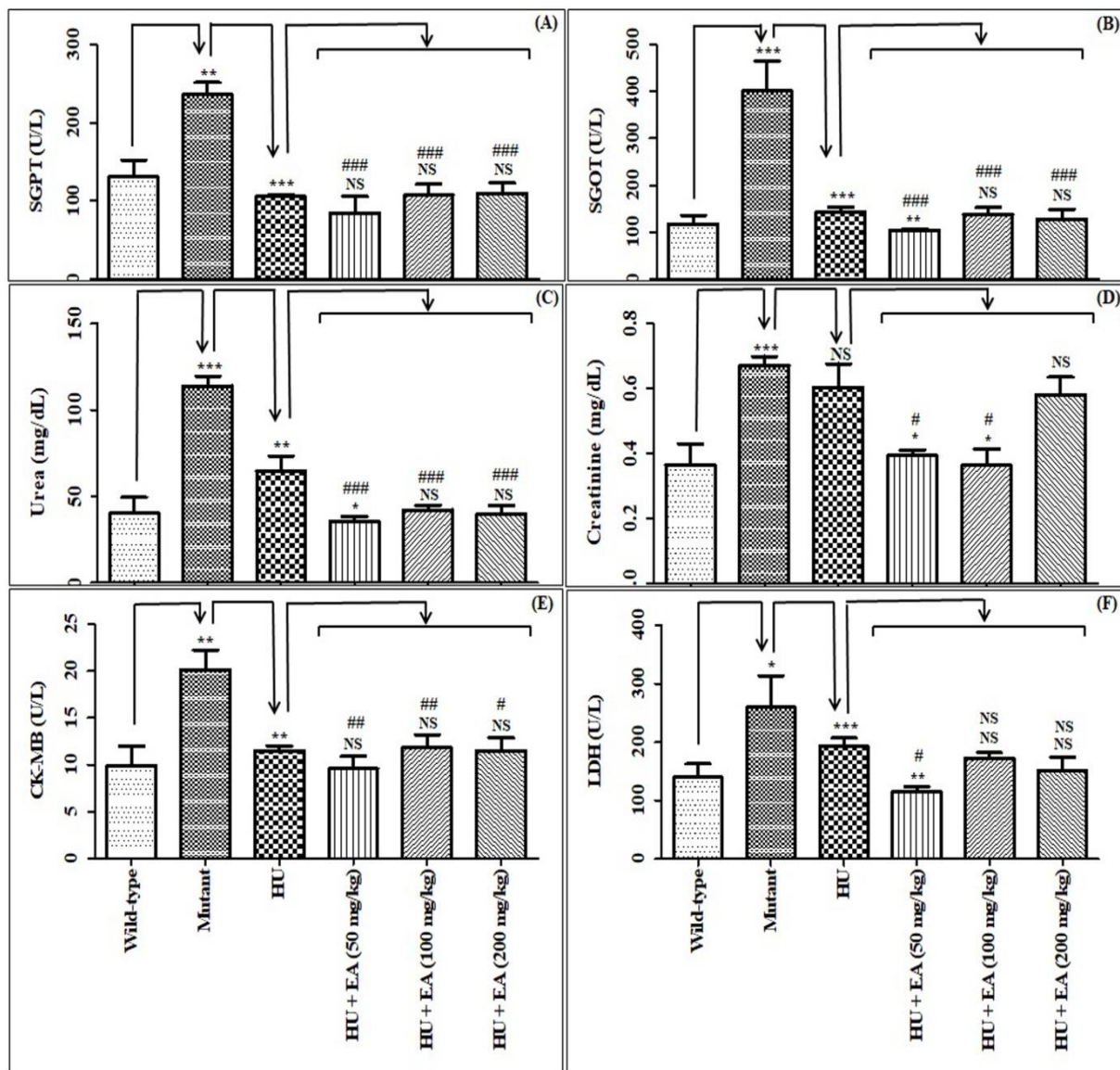


Figure S8. Effect of ellagic acid (EA) upon concomitant treatment with HU on the following parameters: SGPT (A); SGOT (B); urea (C); creatinine (D); CK-MB (E); LDH (F). Data are expressed as mean \pm SEM (n=5). $p < 0.05/0.01/0.001$ denotes statistically significance (*/**/*** or #/###/####). *wild-type vs. mutant/mutant vs. HU/HU vs. HU+EA. #mutant vs. HU+EA. NS denotes not statistically significant.

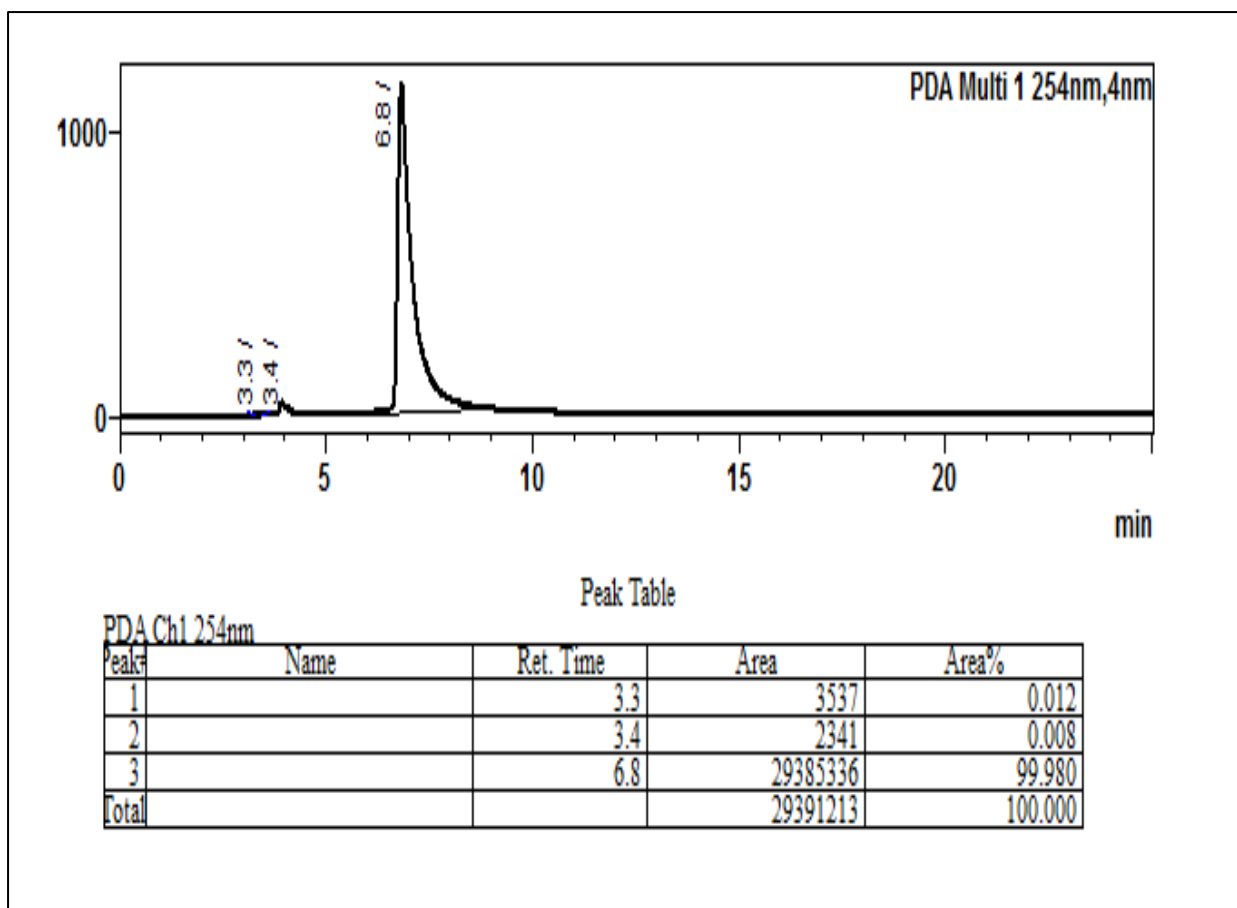


Figure S9. Chromatographic purity of ellagic acid by HPLC.

DETAILED METHODOLOGY

Chemicals and reagents

HU (purity $\geq 98\%$), *p*-hydroxybenzoic acid (purity $\geq 99\%$), sodium metabisulfite (purity $\geq 98\%$), hemin (purity $\geq 95\%$), citrate-phosphate-dextrose solution with adenine (CPDA), Hank's Balanced Salt Solution (HBSS), MDA (purity $\geq 98\%$), GSH (purity $> 98\%$), hypoxanthine (purity $\geq 99\%$), L-arginine (purity $\geq 98\%$), L-proline (purity $\geq 99\%$), and triton X-100 were purchased from Sigma-Aldrich. Nitrotyrosine (purity $\geq 98\%$) was acquired from Cayman. Phosphate buffered saline (PBS), EDTA disodium salt, and heparin were procured from Himedia. Acetonitrile and formic acid (MS-grade) were purchased from Thermo Fisher. Any other chemicals were of bio-reagent grade or above. Ultrapure and distilled water (Make: Merck-Millipore; Model: Direct-Q3 System) were used for analysis and animals, respectively.

ERK1/2 (lot # 461212082) antibody was procured from Sigma-Aldrich. p-IkB α (lot # L2319) and p-NF- κ B p65 (lot # K1219) antibodies were acquired from Santacruz. Bcl-2 (lot # TA257795) antibody was obtained from Thermo Fisher.

Ex vivo studies

- **Ethical approval.** To perform *ex vivo* studies, collected blood from SCD patients' (donors) upon prior approval from the 'Institutional Human Ethics Committee' of Government Medical College, Jammu, India (Approval number: IEC/GMC/Cat A/2020/267). Regarding SCD patients, no separate genetic study was done to assess the number of mutations and the chain in which mutation(s) occurred for differentiating among SCD type including SCA.

- **Effect of ellagic acid on anti-sickling activity.** The anti-sickling activity of ellagic acid was performed using our earlier reported protocol.¹ Briefly, the SCD patient's blood was collected in a centrifuge tube containing CPDA buffer and diluted in HBSS. The counting of cells was done using a hemocytometer (Make: Rohem; Model: IS10269/BS749). RBC (5.0×10^4 cells) were seeded in a 96-well plate and pre-treated with ellagic acid (12.5 to 100 μM). The plate was incubated in a 5% CO_2 incubator (37° C, 1 h) and then treated with sickling inducing agent. A combination of cobalt chloride (1.5 mM) and sodium metabisulphite (0.5 %, w/v) was used as sickling inducing agent, and the sample without inducing agent served as the control. Finally, cells were analyzed under a light microscope (Make: Magnus Opto Systems; Model: INVI). The assay was performed in triplicate using *p*-hydroxybenzoic acid (50 μM) as a positive control. Cells treated only with the inducing agent served as a negative control (100 % sickling) and were used to calculate the inhibition of sickling.
- **Effect of ellagic acid on polymerization inhibition.** To assess polymerization inhibition by ellagic acid, we adopted our previously reported protocol using SCD patients' blood.² Concisely, a specific amount of donor blood and above-mentioned sickling-inducing agent was poured into a 96-well plate, treated with ellagic acid (12.5 to 100 μM), and measured the absorbance (700 nm) using the plate reader every 2 min for 30 min. The sample with an equal volume of PBS in place of ellagic acid solution served as a control. Assay was performed in triplicate using HU (50 μM) as a reference compound. Finally, the difference in final and initial absorbance to time was used to calculate the rate of polymerization.
- **Effect of ellagic acid on hemolytic activity.** We determined any influence of ellagic acid on the hemolytic activity using SCD patients' blood following our established protocol.³ Briefly, donor blood in CPDA buffer was collected and centrifuged (6082 g, 10 min, 4 °C) to obtain RBC, which was then washed and diluted with PBS. After that, mixed the diluted RBC and PBS containing ellagic acid (0.01 to 1 mg/mL) in microcentrifuge tubes, incubated (37°C, 30 min) in the shaking water bath (Make: Remi Elektrotechnik; Model: RSB-12), did centrifugation (6082 g, 10 min, 4°C), and measured the absorbance (540 nm) by the plate reader. Assay was performed in triplicate using 1% triton X-100 in PBS (100 % hemolysis) and PBS (0 % hemolysis) as a positive and negative control, respectively. The % hemolysis was calculated using the following formula:

$$\% \text{ Hemolysis} = \frac{(\text{Absorbance}_{\text{sample}} - \text{Absorbance}_{0\%})}{(\text{Absorbance}_{100\%} - \text{Absorbance}_{0\%})} \times 100$$

In vivo studies

- **Animal model.** Animal experiments were performed using sickle cell transgenic mice *Hba^{tm1Paz}Hbb^{tm1TowTg}* (HBA-HBBs) 41Paz/J (Jax: 003342), Berkeley model of Sickle Cell Disease (SCD). Sickle mice are homozygous null allele for murine α [*Hba^(-/-)*] and β [*Hbb^(-/-)*] globin genes with sickle transgene Tg (Hu-miniLCR $\alpha 1^{\text{G}}\gamma^{\text{A}}\delta\beta^{\text{S}}$) which expresses the haematological and histopathological characteristics of human sickle cell anaemia disease. The non-sickle mice are homozygous for murine α [*Hba^(-/-)*] globin null allele with sickle transgene, but heterozygous/wildtype for murine β (*Hbb^{+/-}/Hbb^{+/+}*) globin gene which inhibits the sickling effect. Male mice homozygous for *Hba^(-/-)*, *Hbb^(-/-)*, and Tg (*Hba-Hbb^S*)^{Tg/Tg} were bred to female mice homozygous for *Hba^(-/-)*, heterozygous for *Hbb^(+/-)*, and hemizygous for Tg (*Hba-Hbb^S*)^{Tg/0} to produce the experiment animals. All mice were genotyped for *Hba^{tm1Paz}*, *Hbb^{tm1Tow}*, and Tg (HBA-HBBs)41Paz/J genes as per the protocols of Jackson Laboratory with standardised PCR and RT-PCR cyclic

conditions to obtain the sickle (Mutant) and non-sickle (Wildtype/Heterozygous) mice (Table S1 to Table S3; Figure S10). All mice used in this experiment were in the age group of 4-5 months and maintained in IVC cages under standard laboratory conditions and a pellet diet with free access to water. The animal study was executed following 'Committee for Control and Supervision of Experiments on Animals (CCSEA)' (New Delhi, India) guidelines.

- **Ethical approval.** To perform *in vivo* studies in *mice model*, took necessary approval from our 'Institutional Animal Ethics Committee' (Approval number: 80/280/2/2022).

Table S1. List of primers used for genotyping of *Hba*, *Hbb*, and *Tg* (*Hba-Hbb^S*)

| Primers and Probes | T _a (°C) | Size (bp) |
|---|---------------------|-----------|
| Tg (HBA-HBBs) 41Paz (5'–3') | | |
| Internal Control Primers | | |
| FP: CAC GTG GGC TCC AGC ATT | 60.0 | -- |
| RP: TCA CCA GTC ATT TCT GCC TTT G | | |
| Probe: Fam-CCA ATG GTC GGG CAC TGC TCA A | | |
| Transgene Primers | | |
| FP: GGA ATG GAA AGG AAA GTG AAT ATT TG | 60.0 | -- |
| RP: GCT GTC TCC TAG CAA CGA CTT CT | | |
| Probes: Hex-CCC ACC TCC AGT GTA ACT GCC TAG TCT TTC ATA A | | |
| Hbb < tm1Tow (5' – 3') | | |
| Common FP: CAG ACT CAC CCT GAA GTT CTC | 60.0 | 164 |
| Wild-type RP: TGA ATC ACT TGG ACA GCC TC | | |
| Wild-type Probe: Hex-ACC TTT GCC AGC CTC AGT GAG C | | |
| Mutant RP: CGG TGG ATG TGG AAT GTG T | | 98 |
| Mutant Probe: Fam-CTT GTG TAG CGC CAA GTG CCC | | |
| Hba < tm1Paz > (5' – 3') | | |
| Wild-type FP: GAC CTA CTT CCC TCA CTT TGA TG | 60.0 | 262 |
| Wild-type RP: CAC TAT GTT CCC TGC CTT GG | | |
| Mutant FP: ATA GAT GGG TAG CCA TTT AGA TTC C | | 481 |
| Mutant RP: CCG GGT TAT AAT TAC CTC AGG TC | | |

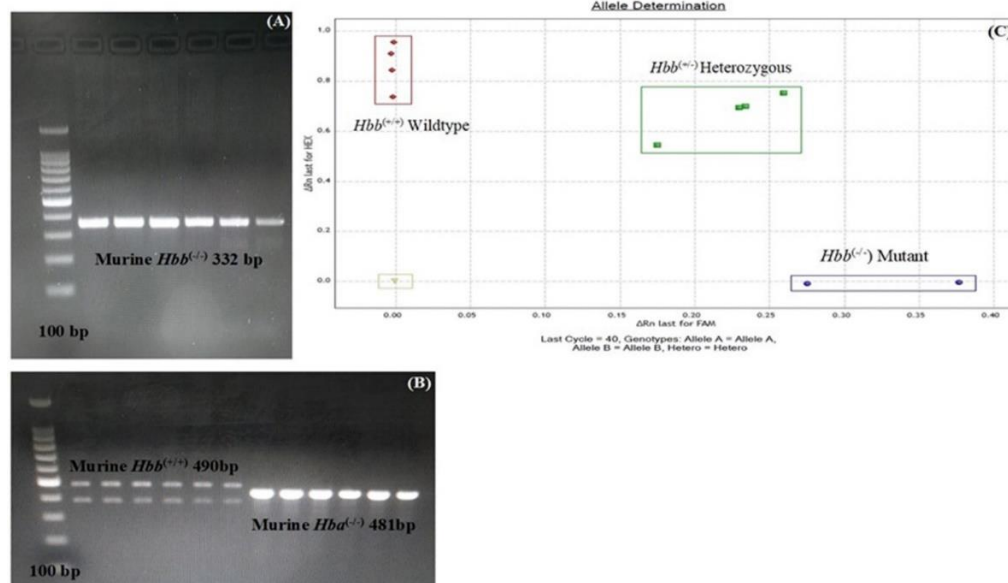
Footnote: FP, forward primer; RP, reverse primer.

Table S2. PCR reaction mixture composition for *Hba*, *Hbb*, and Tg (*Hba-Hbb^S*)

| Components and its Concentration | Volume (μL) |
|--|--------------------------|
| PCR/qPCR Master Mix- 2X | 7.5 |
| Primer – Forward and Reverse - 0.5 μM | 0.7 |
| Probes - 0.2 μM | 0.3 |
| DNA (50 ng/ μL) | 1.5 |
| Nucleus Free water | 3.4 - 4.5 |
| Total | 15 |

Table S3. PCR and RT-PCR reaction conditions for *Hba*, *Hbb*, and Tg (*Hba-Hbb^S*)

| Process | <i>Hba</i> gene | | <i>Hbb</i> and Tg (<i>Hba-Hbb^S</i>) gene | |
|----------------------|-----------------|----------|---|----------|
| | Temperature | Duration | Temperature | Duration |
| Initial denaturation | 95°C | 3 min | 95°C | 2 min |
| Cyclic denaturation | 95°C | 30 s | 95°C | 10 s |
| Primer annealing | 60°C | 30 s | 60°C | 15 s |
| Primer extension | 72°C | 30 s | | |
| No. of cycles | 35 | | 40 | |
| Final extension | 72°C | 5 min | - | - |
| Hold | 4°C | ∞ | - | - |

**Figure S10.** PCR amplicons of mutant alleles of *Hba* and *Hbb* genes (A); wild-type alleles of *Hba* and *Hbb* genes (B); allele discrimination of murine *Hbb* gene using probes (C).

- **Effect of concomitant administration of ellagic acid with HU on various disease pathophysiological conditions of SCD**

- **Study design.** Studies were carried out using a mice model (mutant/homozygous). The dose of HU was 600 mg/kg, which was selected based on evidence to cause a significant change in the hematological profile.⁴ The experimental dose of ellagic acid was chosen from 50 to 200 mg/kg based on the literature reports on any biological activities.^{5, 6} Both the candidates were given orally using a common vehicle for dose preparation, i.e., an aqueous suspension containing Na-CMC (0.25 %, w/v). The dose-volume was 10 mL/kg. A total of twenty-five animals (25 to 30 g of body weight) were

randomly divided into five experimental groups containing five animals/group: Group-1: (mutant) vehicle only; Group-2: HU (600 mg/kg) alone; Group-3: HU (600 mg/kg) + ellagic acid (50 mg/kg); Group-4: HU (600 mg/kg) + ellagic acid (100 mg/kg); Group-5: HU (600 mg/kg) + ellagic acid (200 mg/kg). We also included another vehicle control group (wild-type) containing five animals. HU and ellagic acid were administered for ten consecutive days. At the end of the experiment (on the 11th day), mice were allowed to move on a Rota-rod instrument (Make: Ugo Basile; Model: 73690) for 2 h to cause hypoxia for the induction of sickling. Animals were then used to determine analgesic activity. After that, blood samples from each animal were collected into a microcentrifuge tube containing the following solutions: (i) CPDA buffer (14%, v/v): To investigate anti-sickling activity; (ii) an aqueous solution of heparin (5 IU/L): To evaluate the hematological parameters. Then, blood samples containing heparin were centrifuged (6082 g, 10 min, 4°C) to obtain plasma for determining biochemical markers, cytokines profiles, and P-selectin levels. After the plasma collection, RBC lysate (100 µL/mL) was prepared using lysis buffer to estimate markers like HbF. Then, animals were sacrificed using euthanasia (CO₂) followed by cervical dislocation. Next, dissected the animals, collected the organs (spleen and heart), washed with normal saline, blotted dry, and weighed. A part of the spleen was taken and fixed in neutral buffered formalin (10%, v/v) for histopathological examination. Heart and the remaining spleen, were snap-frozen (liquid nitrogen) and stored (-80°C) for Western blotting (WB). The obtained samples were studied as described below.

- **Effect on analgesic activity.** Analgesic activity was evaluated according to our previously reported procedure.⁷ In brief, animals were placed on a hot plate analgesiometer (Make: Ugo Basile; Model: 57390), which was set at 55 ± 1°C. Paw withdrawal time for each mouse against the thermal stimuli was considered reaction time, and the maximum reaction time was set at 30 s to avoid any paw injury.
- **Effect on anti-sickling activity.** To examine the anti-sickling activity of ellagic acid in the presence of HU, we performed the study using the protocol mentioned above, except for mice blood instead of SCD patient's blood, and there was no requirement to add the inducing agent here.
- **Effect on RBC, Hb, platelet, neutrophil, and HbF levels.** The level of RBC, Hb, platelet, and neutrophil in mice blood was estimated using an automated hematology analyzer (Make: Sysmex; Model: XT1800i). The level of HbF was measured in RBC lysates using ELISA kits (MyBioSource) according to the manufacturer's instructions.
- **Effect on nitric oxide, L-arginine, and L-proline levels.** The nitric oxide content in spleen tissue homogenates was determined using Griess protocol. Homogenate (100 mg/mL) was prepared in PBS (10 mM, pH 7.4), and quantitation was done using sodium nitrate (12.5 to 200 µM) (Jang et al., 2014). To measure the plasma levels of L-arginine and L-proline, the samples (10 µL each) were processed by adding acetonitrile (190 µL), vortex mixed (2 min), centrifuged (18626 g, 10 min), decanted into inner vials, and injected onto LC-MS/MS (Make: Thermo Fisher Scientific; Model: TSQ Endura) (Table S4 and Table S5).
- **Effect on nitrotyrosine and hypoxanthine levels.** To measure nitrotyrosine and hypoxanthine levels in spleen tissue, each homogenate was prepared at 100 mg/mL using methanol: water (50:50, v/v), centrifuged (18626 g, 10 min),

filtered (0.22 μm), poured into inner vials, and injected onto LC-MS/MS (Table S4 and Table S5).

- **Effect on MDA and GSH levels.** MDA content and GSH level in the RBC lysate as well as spleen tissue homogenate were assessed using our earlier reported protocol.^{8, 9} To measure MDA content, RBC lysate/tissue homogenate was prepared using an aqueous KCl solution (1.15%, w/v). To determine GSH content, RBC lysate/tissue homogenate was prepared in sodium phosphate buffer (100 mM) containing EDTA (5 mM) and *o*-phthalaldehyde (1 mg/mL).
- **Effect on hemin level.** To measure hemin levels in spleen tissue, each homogenate was prepared at 100 mg/mL using methanol: water (50:50, v/v), centrifuged (18626 g, 10 min), filtered (0.22 μm), poured into inner vials, and injected onto LC-MS/MS (Table S4).
- **Effect on TNF- α , IL-1 β , GM-CSF and P-selectin levels.** The plasma level of TNF- α (RayBiotech), IL-1 β (RayBiotech), and GM-CSF (BT Laboratory) were quantified using ELISA kits as per the manufacturer's protocol.
- **Effect on spleen histopathology.** To assess histological alterations in the spleen, we adopted our previously reported protocol for hematoxylin and eosin (H&E) staining of tissue.^{10, 11} Briefly, spleen tissue was fixed (10 % neutral buffered formalin solution), embedded in paraffin, sectioned by microtome (around 5 μm of thickness), dehydrated using graded solvent composition (water: ethanol), stained (H&E dye), and observed under a light microscope (Make: Magnus Opto Systems; Model: INVI). The scoring was done using various parameters to demonstrate spleen injury grades: normal (zero), mild (one), moderate (two), and severe (five and above).¹²
- **Effect on NF- κB , I $\kappa\text{B}\alpha$, ERK1/2, and Bcl-2 expressions.** WB was done to assess the protein expression of NF- κB , I $\kappa\text{B}\alpha$, MAPKK, ERK1/2, and Bcl-2, in spleen tissue and CYP2J2 in cardiac tissue using our previously reported protocol.^{2, 9, 10, 13} Briefly, RIPA buffer with a protease inhibitor cocktail: sodium orthovanadate (0.5 mM), PMSF (2 mM), and sodium fluoride (50 mM) was used to prepare the tissue homogenate, which was then used to estimate the protein level following the Bradford method. The protein was separated using SDS-PAGE and then transferred to the PVDF membrane (100 volts, 120 min, 4 $^{\circ}\text{C}$). The membrane was blocked (2 h, room temperature) with 3% BSA to prevent non-specific antibody binding. After that, the membrane was treated with the respective primary antibodies (12 h, 4 $^{\circ}\text{C}$). Following incubation, the membrane was rinsed thrice with Tris-buffered saline before being further incubated with a chemiluminescent secondary antibody (1 h, room temperature). The membrane was rewashed with Tris-buffered saline, and imaging was done using the Chemidoc imaging system (Make: Syngene; Model: G: BOX, XT-4). Densitometry was performed using Image J software.
- **Effect on SGPT, SGOT, urea, creatinine, CK-MB, and LDH levels.** The plasma level of serum glutamic pyruvic transaminase (SGPT), serum glutamic oxaloacetic transaminase (SGOT), urea, creatinine, creatine kinase-myocardial band (CK-MB), and lactate dehydrogenase (LDH) were measured using an automated biochemical analyzer (Make: Erba Mannheim; Model: EM360).

Table S4. LC-MS/MS conditions for the quantification of hypoxanthine, L-arginine, and hemin in plasma/spleen tissue

| Parameters | Conditions |
|---------------------------------------|--|
| LC conditions | |
| Column | ZIC HILIC (50×2.1 mm, 5 µm) |
| Elution | Isocratic |
| Mobile phase | Ammonium formate in water (10 mM): acetonitrile: 50:50, v/v |
| Flow rate | 0.3 mL/min |
| Column temperature | 45 °C |
| Autosampler temperature | 15 °C |
| Retention time of hypoxanthine | ~0.4 min |
| Retention time of L-arginine | ~1.2 min |
| Retention time of hemin | ~0.5 min |
| Run time | 2 min |
| MS conditions | |
| Scan type | SRM |
| Source | H-ESI |
| Ion polarity | Negative |
| Ion voltage (V) | 2500 |
| Vaporizer temperature (°C) | 300 |
| Ion transfer tube temperature (°C) | 250 |
| Sheath gas (Arbitrary scale) | 30 |
| Auxiliary gas (Arbitrary scale) | 10 |
| CID gas (mTorr) | 1.5 |
| Dwell time per transition (ms) | 13 |
| RF lens for hypoxanthine (V) | 122 |
| RF lens for L-arginine (V) | 105 |
| RF lens for hemin (V) | 288 |
| Q1 resolution (FWHM) | 0.7 |
| Q3 resolution (FWHM) | 0.7 |
| Collision energy for hypoxanthine (V) | 15 |
| Collision energy for L-arginine (V) | 23 |
| Collision energy for hemin (V) | 25 |
| Ion transition for hypoxanthine (m/z) | 135.0 → 92.2 |
| Ion transition for L-arginine (m/z) | 175.1 → 70.3 |
| Ion transition for hemin (m/z) | 650.0 → 570.1 |

Table S5. LC-MS/MS conditions for the quantification of nitrotyrosine and L-proline in plasma/spleen tissue

| Parameters | Conditions |
|--|--|
| LC conditions | |
| Column | ZIC HILIC (50x2.1 mm, 5 μ m) |
| Elution | Isocratic |
| Mobile phase | Ammonium formate in water (10 mM): acetonitrile: 50:50, v/v |
| Flow rate | 0.3 mL/min |
| Column temperature | 45 °C |
| Autosampler temperature | 15 °C |
| Retention time of nitrotyrosine | ~0.4 min |
| Retention time of L-proline | ~0.5 min |
| Run time | 2 min |
| MS conditions | |
| Scan type | SRM |
| Source | H-ESI |
| Ion polarity | Positive |
| Ion voltage (V) | 3500 |
| Vaporizer temperature (°C) | 300 |
| Ion transfer tube temperature (°C) | 250 |
| Sheath gas (Arbitrary scale) | 30 |
| Auxiliary gas (Arbitrary scale) | 10 |
| CID gas (mTorr) | 1.5 |
| Dwell time per transition (ms) | 13 |
| RF lens for nitrotyrosine (V) | 118 |
| RF lens for L-proline (V) | 74 |
| Q1 resolution (FWHM) | 0.7 |
| Q3 resolution (FWHM) | 0.7 |
| Collision energy for nitrotyrosine (V) | 10 |
| Collision energy for L-proline (V) | 23 |
| Ion transition for nitrotyrosine (m/z) | 227.1 \rightarrow 181.1 |
| Ion transition for L-proline (m/z) | 116.2 \rightarrow 70.3 |

- **Effect of ellagic acid on the pharmacokinetics of HU (*in vivo*)**

- **Study design.** The pharmacokinetic interaction study of HU in the presence or absence of ellagic acid was performed using a mice model (Wild/heterozygous) using our earlier reported protocol.^{8, 14} The dose of both HU and ellagic acid was 100 mg/kg. The route of administration, vehicle, and dose-volume were the same as mentioned above. A total of thirty overnight (10 h) fasted animals were randomly divided into six groups containing five animals/group. Each study arm consisted of three animal groups to accomplish a sparse sampling procedure for blood collection.¹⁵ Study arms were as follows: Group-1: HU alone; Group-2: HU + ellagic acid. Ellagic acid was administered at 0.5 h before HU dosing to observe the maximum effect. After a single oral dose of HU administration, blood samples were collected from the retro-orbital plexus at 0 h (pre-dose), 0.083 h, 0.25 h, 0.5 h, 1 h, and 2 h into microcentrifuge tubes containing anti-coagulant. Then, each blood sample was centrifuged (6082 g, 10 min) to separate plasma (50 μ L each) and stored (-80°C) till analysis.
- **Bioanalysis.** Quantitation of HU in plasma was carried out using our earlier developed LC-MS/MS-based bioanalytical method.¹⁻⁴ Sample processing was done using acetonitrile containing methylurea as an internal standard, and quantitation of HU in mice plasma was done using a matrix-match calibration curve (156 to 80000 ng/mL).
- **Pharmacokinetic analysis.** Plasma concentration data of HU at the specific time points were fitted to the non-compartmental model to calculate various pharmacokinetic parameters (PK solution, Summit Research Services, USA).

- **Statistical analysis**

Statistical significance was determined using Analysis of variance (ANOVA) followed by Tukey's test (GraphPad Prism). For the pharmacokinetic interaction, statistical evaluation was done using an unpaired Student's t-test (QuickCalcs, GraphPad). *p*-value of less than 0.05, 0.01, and 0.001 was considered statistically significant.

References

- [1] Gour, A., Kotwal, P., Dogra, A., Kour, D., Dhiman, S., Kumar, A., Digra, S. K., Kumar, A., Singh, G., and Nandi, U. (2022) Investigating the Potential Use of Andrographolide as a Coadjuvant in Sickle Cell Anemia Therapy, *ACS Omega*. 7, 12765-12771. <https://doi.org/10.1021/acsomega.1c07339>.
- [2] Gour, A., Kour, D., Dogra, A., Manhas, D., Wazir, P., Digra, S. K., Kumar, A., and Nandi, U. (2022) Epicatechin exerts dual action to shield sickling and hydroxyurea-induced myelosuppression: Implication in sickle cell anemia management, *Toxicol. Appl. Pharmacol.* 449, 116113. <https://doi.org/10.1016/j.taap.2022.116113>.
- [3] Gour, A., Dogra, A., Kour, D., Singh, G., Kumar, A., and Nandi, U. (2021) Effect of Concomitant Hydroxyurea Therapy with Rutin and Gallic Acid: Integration of Pharmacokinetic and Pharmacodynamic Approaches, *ACS Omega*. 6, 14542-14550. <https://doi.org/10.1021/acsomega.1c01518>.
- [4] Gour, A., Dogra, A., Wazir, P., Singh, G., and Nandi, U. (2020) A highly sensitive UPLC-MS/MS method for hydroxyurea to assess pharmacokinetic intervention by phytotherapeutics in rats, *J. Chromatogr. B*. 1154, 122283. <https://doi.org/10.1016/j.jchromb.2020.122283>.
- [5] El-Shitany, N. A., El-Bastawissy, E. A., and El-desoky (2014) Ellagic acid protects against carrageenan-induced acute inflammation through inhibition of nuclear factor kappa B, inducible cyclooxygenase and proinflammatory cytokines and

- enhancement of interleukin-10 via an antioxidant mechanism, *Int. Immunopharmacol.* 19, 290-299. <https://doi.org/10.1016/j.intimp.2014.02.004>.
- [6] Lee, J. H., Won, J. H., Choi, J. M., Cha, H. H., Jang, Y. J., Park, S., Kim, H. G., Kim, H. C., and Kim, D. K. (2014) Protective effect of ellagic acid on concanavalin A-induced hepatitis via Toll-like receptor and mitogen-activated protein kinase/nuclear factor κ B signaling pathways, *J. Agric. Food Chem.* 62, 10110-10117. <https://doi.org/10.1021/jf503188c>.
- [7] Sharma, A., Magotra, A., Dogra, A., Rath, S. K., Rayees, S., Wazir, P., Sharma, S., Sangwan, P. L., Singh, S., Singh, G., and Nandi, U. (2017) Pharmacokinetics, pharmacodynamics and safety profiling of IS01957, a preclinical candidate possessing dual activity against inflammation and nociception, *Regul. Toxicol. Pharmacol.* 91, 216-225. <https://doi.org/10.1016/j.yrtph.2017.10.033>.
- [8] Bhatt, S., Sharma, A., Dogra, A., Sharma, P., Kumar, A., Kotwal, P., Bag, S., Misra, P., Singh, G., Kumar, A., and Nandi, U. (2022) Glabridin attenuates paracetamol-induced liver injury in mice via CYP2E1-mediated inhibition of oxidative stress, *Drug Chem. Toxicol.* 45, 2352-2360. <https://doi.org/10.1080/01480545.2021.1945004>.
- [9] Gour, A., Dogra, A., Verma, M. K., Bhardwaj, M., Kour, D., Jamwal, A., Gorain, B., Kumar, M., Vij, B., Kumar, A., and Nandi, U. (2022) Ayurveda-based phytochemical composition attenuates lung inflammation and precipitates pharmacokinetic interaction with favipiravir: an in vivo investigation using disease-state of acute lung injury, *Nat. Prod. Res.* 1-8. <https://doi.org/10.1080/14786419.2022.2150620>.
- [10] Dogra, A., Gupta, D., Bag, S., Ahmed, I., Bhatt, S., Nehra, E., Dhiman, S., Kumar, A., Singh, G., Abdullah, S. T., and Nandi, U. (2021) Glabridin ameliorates methotrexate-induced liver injury via attenuation of oxidative stress, inflammation, and apoptosis, *Life Sci.* 278, 119583. <https://doi.org/10.1016/j.lfs.2021.119583>.
- [11] Dogra, A., Kour, D., Gour, A., Bhardwaj, M., Bag, S., Dhiman, S. K., Kumar, A., Singh, G., and Nandi, U. (2022) Ameliorating effect of rutin against diclofenac-induced cardiac injury in rats with underlying function of FABP3, MYL3, and ANP, *Drug Chem. Toxicol.* 1-12. <https://doi.org/10.1080/01480545.2022.2069804>.
- [12] Al-Quraishy, S., Murshed, M., Delic, D., Al-Shaebi, E., Qasem, M., Mares, M., and Dkhil, M. (2020) Plasmodium chabaudi-infected mice spleen response to synthesized silver nanoparticles from Indigofera oblongifolia extract, *Lett. Appl. Microbiol.* 71, 542-549. <https://doi.org/10.1111/lam.13366>.
- [13] Bhatt, S., Kumar, V., Dogra, A., Ojha, P. K., Wazir, P., Sangwan, P. L., Singh, G., and Nandi, U. (2021) Amalgamation of in-silico, in-vitro and in-vivo approach to establish glabridin as a potential CYP2E1 inhibitor, *Xenobiotica.* 51, 625-635. <https://doi.org/10.1080/00498254.2021.1883769>.
- [14] Sharma, A., Magotra, A., Rath, S. K., Wazir, P., Nandi, U., Koul, S., Sangwan, P. L., Gupta, A. P., and Singh, G. (2018) In-vitro and in-vivo pharmacokinetics of IS01957, p-coumaric acid derivative using a validated LC-ESI-MS/MS method in mice plasma, *J. Pharm. Investig.* 48, 565-574. <https://doi.org/10.1007/s40005-017-0350-8>.
- [15] Manhas, D., Mir, K. B., Tripathi, N., Bharti, S., Dhiman, S., Wazir, P., Sharma, D. K., Goswami, A., and Nandi, U. (2022) Rottlerin promotes anti-metastatic events by ameliorating pharmacological parameters of paclitaxel: An in-vivo investigation in the orthotopic mouse model of breast cancer, *Chem. Biol. Interact.* 366, 110109. <https://doi.org/10.1016/j.cbi.2022.110109>.